

**This item is the archived peer-reviewed author-version of:**

Monitoring the impact of the indoor air quality on silver cultural heritage objects using passive and continuous corrosion rate assessments

**Reference:**

't Hart Lucy, Storme Patrick, Anaf Willemien, Nuyts Gert, Vanmeert Frederik, Dorriné Walter, Janssens Koen, De Wael Karolien, Schalm Olivier.- Monitoring the impact of the indoor air quality on silver cultural heritage objects using passive and continuous corrosion rate assessments

Applied physics A: materials science & processing - ISSN 0947-8396 - 122:10(2016), 923

Full text (Publisher's DOI): <http://dx.doi.org/doi:10.1007/S00339-016-0456-2>

To cite this reference: <http://hdl.handle.net/10067/1355110151162165141>

# Monitoring the Impact of the Indoor Air Quality on Silver Cultural Heritage Objects using Passive and Continuous Corrosion Rate Assessments

**Lucy 't Hart<sup>1\*</sup>, Patrick Storme<sup>1</sup>, Willemien Anaf<sup>2</sup>, Gert Nuyts<sup>3</sup>, Frederik Vanmeert<sup>3</sup>, Walter Dorriné, Koen Janssens<sup>3</sup>, Karolien de Wael<sup>3</sup> and Olivier Schalm<sup>1</sup>**

<sup>1</sup>University of Antwerp, Faculty of Design Sciences, Conservation Studies, Blindestraat 9, 2000 Antwerp, +3232137134, [Pieternel.tHart@uantwerpen.be](mailto:Pieternel.tHart@uantwerpen.be)\*

<sup>2</sup>Royal Museum of the Armed Forces and of Military History Brussels, Scientific Research, Jubelpark 3, 1000 Brussels.

<sup>3</sup>University of Antwerp, Faculty of Science, Department of Chemistry, AXES, Groenenborgerlaan 171, 2020 Antwerp.

\* Corresponding author's email address, phone/fax

**Keywords:** indoor air quality, heritage, preventive conservation, corrosion monitoring system, silver

## Abstract

There is a long tradition in evaluating industrial atmospheres by measuring the corrosion rate of exposed metal coupons. The heritage community also uses this method, but the interpretation of the corrosion rate often lacks clarity due to the low corrosivity in indoor museum environments. This investigation explores the possibilities and drawbacks of different silver corrosion rate assessments. The corrosion rate is determined by three approaches: (1) chemical characterization of metal coupons using analytical techniques such as electrochemical measurements, SEM-EDX, XRD and  $\mu$ -Raman spectroscopy, (2) continuous corrosion monitoring methods based on electrical resistivity loss of a corroding nm-sized metal wire and weight-gain of a corroding silver coated quartz crystal, and (3) characterizing the visual degradation of the metal coupons. This study confirms that subtle differences in corrosivity between locations inside a museum can be determined on condition that the same corrosion rate assessment is used. However, the impact of the coupon orientation with respect to the prevailing direction of air circulation can be substantially larger than the impact of the coupon location.

## 1. Introduction

Heritage caretakers have the challenging task to create a suitable environment for the safekeeping of object collections. Their aim is to achieve an overall degradation rate that is as low as possible. Generally, one attempts to answer the following three questions:

- (1) how dangerous is the environment to the collection
- (2) when should mitigation actions be applied
- (3) how are these actions to be evaluated

In order to answer them, it is a common practice to monitor environmental parameters (e.g. temperature (T), relative humidity (RH), and intensity of visible light ( $L_v$ )). The impact of such parameters on a collection is usually estimated using predefined target values [1,2]. Indoor air pollution is another crucial parameter that affects the overall transformation rate of many heritage materials [3]. However, indoor pollution concentrations are close to the detection limit of many pollution sensors. For example, silver tarnishes within a period of days to months when it is in contact with ppb-amounts of hydrogen sulphide ( $H_2S$ ); Such concentrations are very hard to measure with inexpensive sensors [4]. Moreover, synergetic and antagonistic effects complicate the prediction of silver corrosion rates from the environmental parameters [5-7].

An alternative way is to measure the corrosion rate of metal coupons [7,8,9] and use this corrosion rate to estimate the corrosivity of an environment [10]. The relation between corrosion rate and the corresponding indoor air quality (IAQ) are described by several norms [11,12]. To evaluate the outcome of metal coupons, the corrosion rate can be assessed in different ways. Conventionally, coulombic reduction is used [9,13]. The change in visual appearance has also been used as a way to determine the corrosion extent [14]. Furthermore, resistance measurements of nm-thick metal wires can monitor metal loss over time (e.g., Cosasco®, AirCorr®) [15-18]. All these corrosion rate assessments use a different quantity to determine the corrosion extent, hampering the conversion of the different types of corrosion rates to other types. In addition, parameters such as the orientation of the metal sensor seems to affect the corrosion rate that might interfere with the variation of aggressivity across a room. In this paper, the usefulness of silver sensors to evaluate IAQ will be determined. For this, the possibilities and drawbacks of 4 types of silver corrosion rate assessments will be evaluated. Subsequently, the impact of several parameters on the measurements are assessed.

## 2. Experimental

For this study, several measuring campaigns have been realized to compare the performance of different types of silver sensors. The corrosion rate of metallic silver was determined by two methods. (1) Passive methods determine the average corrosion rates. For this, self-made coupons (i.e. University of Antwerp Coupons, UAC) and Corrosion Classification Coupons (CCC) of Purafil were used. (2) Continuous monitoring methods determine the corrosion rates in real-time. Both an Environmental Condition Monitor (ECM) of Rorhback Cosasco and an OnGuard4000 (OG4) of Purafil were tested. The measuring campaigns were realized in 4 different Belgian institutes. Within these institutes, different types of environments were selected (i.e., outdoor, indoor in galleries and storage facilities, and inside display cases). An overview of the measuring locations is given below (Table I). The present study evaluates the silver sensors with three different approaches (Table I, column I).

1. The first approach, chemical characterization of corrosion layers, investigates how chemical characterization of the corrosion products formed on metal coupons can contribute to the evaluation of the IAQ;
2. The second approach, continuous evaluation of corrosion layers, compares the two continuous monitoring methods, which are subsequently compared to the absolute corrosion values of the passive methods.
3. The third approach, visual characterization of corrosion layers, uses gloss and colour (i.e., two quantitative aspects of visual appearance) of exposed metal coupons in order to study whether these can be used as a corrosion rate indicator by comparing the results to electrochemical measurements. In a second part, the impact of position and orientation of the sensors on the corrosion rates were evaluated.

TABLE I: Three approaches to evaluate IAQ using 4 types of silver sensors. Results were obtained from outdoor environments, outside and inside a display case in a gallery, and in a storage facility in 4 different institutes.

Approach	Silver sensor	Passive	Continuous	Institute	Outdoor	Storage	Gallery	Display	Aim
1. Chemical characterization of corrosion layers	UAC			FIN					<ul style="list-style-type: none"> <li>• Explore contribution chemical characterization with SEM-EDX, XRD, Raman compared to electrochemical measurements</li> <li>• Compare corrosivity of locations</li> </ul>

										in one museum
<b>2. Continuous evaluation of corrosion layers</b>	OG4			ART						<ul style="list-style-type: none"> <li>• Compare commercial sensors</li> <li>• Compare passive and continuous sensors</li> <li>• Compare corrosivity at different institutes</li> </ul>
	ECM			FIN						
				ARM						
	CCC			FIN						
	UAC									
	OG4									
	ECM									
<b>3. Visual characterization of corrosion layers</b>	UAC			FIN						<ul style="list-style-type: none"> <li>• Explore possibilities of colour and gloss as corrosion rate indicator</li> <li>• Explore the impact of position and orientation of the sensors on the corrosion rates</li> <li>• Compare corrosivity between in- and outside a display</li> </ul>
				ARM						
				UMI						

FIN: Royal Museums of Fine Arts of Belgium in Brussels, Belgium

ARM: Royal Museum of the Armed Forces and of Military History in Brussels, Belgium

UMI: UMICORE Silver pavilion in Antwerp, Belgium

ART: Archival library of the Royal Academy of Fine Arts in Antwerp, Belgium

### 2.1. Silver sensors

The four silver sensors mentioned in the second column of Table I determine the corrosion extent by measuring a specific quantity such as the electrical charge needed to reduce all corroded silver, the mass loss of the metal, the mass increase due to corrosion build-up or the loss in metal thickness, etc. These parameters are converted to corresponding corrosion rates (Table II). However, the different corrosion rates in Table II are not identical. Only on the assumption of homogeneous corrosion layers with fixed compositions, it is possible to make conversions between all mentioned corrosion rates in each other. The different sensors are described below:

- Self-made University of Antwerp Coupons (UAC) with a size of 20 × 50 mm were cut from a single sheet of pure silver (0,5 mm thick, Schöne Metals Corporation, Amsterdam, the Netherlands). Such large coupon surface is needed to avoid interference of the accelerated corrosion at the edges. The accelerated corrosion at sharp edges is a commonly occurring phenomenon that might be caused by enhanced electrical fields due to curved surfaces. The following procedure is used to obtain similar surface states. First, the surface at both sides was ground with an Al<sub>2</sub>O<sub>3</sub>-coated polyester fiber rotating wheel. Subsequently, the coupons were rinsed with absolute ethanol with a purity of 99%. Finally, at the moment of exposure the coupons were prepared by gently abrading both sides with a fibreglass brush. The coupons were placed in a 45° angle on an L-shaped Plexiglass stand to allow free airflow on both sides of the coupons. The coupons were exposed for a period of 3 to 9 months, depending on the corrosion rate that is determined visually, based on the discolouration of the coupon. After exposure, the developed corrosion layer was determined by coulombic reduction, by visual and chemical characterization and the average corrosion rate  $\langle r_{\text{corr}} \rangle$  defined in Table II was calculated.
- Corrosion Classification Coupons (CCC, Purafil, Doraville GA, US) are a commercially available passive method. It consists of a clean silver sheet that is mounted on a Plexiglass support panel, positioned approximately 3 mm above the Plexiglass surface. The CCC coupons are exposed for 90 days. Then, the coupons are returned to Purafil where the corrosion rate is being assessed by coulombic reduction which is converted into  $\langle r_{\text{corr}} \rangle$ .

- The continuous method Environmental Condition Monitoring System (ECM, Cosasco, Santa Fe Springs, CA, USA) is equipped with an 'Atmospheric electrical resistivity corrosion sensor 610', which is a 250 nm thick silver sensor. One part of the Ag-track is exposed to the environment and is subject to corrosion; the second part, protected by a coating, acts as a reference. For both parts of the track, the electrical resistivity is measured over time. This corrosion sensor evaluates the environmental corrosivity in terms of the real time value  $r_{tl}$  (Table II).
- The second continuous method used, is the Purafil OnGuard4000® (OG4). It uses a quartz crystal microbalance coated with silver. The corrosion build-up of the silver layer is monitored by measuring the change in mass ( $r_{mi}$  of Table II).

**TABLE II** Overview of different parameters to determine the corrosion extent and corresponding corrosion rate.

Metal corrosion extent	Calculation of the corrosion rate	Reference
Mass-loss ( $r_{corr}$ )	$r_{corr} [\text{mg m}^{-2} \text{a}^{-1}] = \Delta m_m \text{ t}^{-1}$	[19]
	$r_{corr} [\text{mg m}^{-2} \text{a}^{-1}] = i \text{ t}_{red} M \text{ n}^{-1} \text{ F}^{-1} \text{ t}^{-1}$	[19, 21]
Mass increase due to corrosion build-up ( $r_{mi}$ )	$r_{mi} [\text{mg m}^{-2} \text{a}^{-1}] = m_s \text{ t}^{-1}$	[19, 22, 23]
Metal thickness loss ( $r_{tl}$ )	$r_{tl} [\text{nm day}^{-1}] = h_m \text{ t}^{-1}$	[15, 23, 24, 25]

$m_m$ : mass metal (mg);  $i$ : current density ( $\text{mA/m}^2$ );  $t_{red}$ : total reduction time (s);  $M$ : molar mass (g/mol);  $n$ : valence state;  $F$ : Faraday's constant (C/mol);  $m_s$ : mass corrosion compound (mg);  $h_c$ : height corrosion film thickness (nm);  $h_m$ : height metal loss (nm)

## 2.2. Approaches used to determine the extent of corrosion

The extent of corrosion of the different corrosion rate sensors is evaluated using three different approaches (first column, Table I). The approaches are described in the following paragraphs.

### 2.2.1. Chemical characterization of corrosion layers

Electrochemical analyses (i.e. linear sweep voltammetry (LSV) and chronopotentiometry (POT)) were used to perform a chemical speciation of the corrosion products present at the surface of UAC coupons and to determine the surface concentrations of these species. Additional information was obtained by analytical techniques such as scanning electron microscopy equipped with an energy dispersive X-ray detector (SEM-EDX), X-ray diffraction (XRD) and  $\mu$ -Raman spectroscopy.

- **Linear sweep voltammetry (LSV):** This was performed with a PalmSens3<sup>®</sup> potentiostat (PalmSens BV) controlled with the PSTrace software. A three-electrode cell filled with 8 mL of a 0,1 M  $\text{Na}_3\text{H}(\text{CO}_3)_2$  electrolyte was provided with an aperture of 5 mm diameter (i.e., 0,2  $\text{cm}^2$ ), giving access to the coupon surface (working electrode). A mercury sulphate electrode (MSE) and a 2 mm platinum (Pt) tube were used as the reference and counter electrode respectively. LSV was performed in the -0,4 V to -1,9 V/MSE range at a scan rate of 5  $\text{mV s}^{-1}$ .
- **Chronopotentiometry (POT):** This was performed in a similar setup as described for LSV. A constant current of -100  $\mu\text{A}$  was applied (i.e., for an area of 0,2  $\text{cm}^2$  this corresponds with a current density of -500  $\mu\text{A cm}^{-2}$ ). The total reduction time ( $t_{red}$ ) in seconds was determined by

calculating the first derivative of the chronopotentiogram by applying a 25-point linear/quadratic Savitsky-Golay filter. On the assumption that only  $\text{Ag}_2\text{S}$  was being formed as corrosion product, Faraday's law of electrolysis was used to determine the mass loss of the metal.

- **Scanning electron microscopy (SEM-EDX):** A Field Emission Gun - Environmental SEM-EDX (FEG-ESEM-EDX, FEI Quanta 250) was used to inspect the surfaces. Secondary Electron (SE) images, X-ray spectra and element maps were collected using an accelerating voltage of 20 kV. The take-off angle is  $30^\circ$ , the working distance is 10 mm, the current differs between 0.2 and 6 nA and the chamber pressure is  $10^{-4}$  Pa.
- **X-ray diffraction (XRD):** This analysis was performed using a copper X-ray microsource (50 kV, 600  $\mu\text{A}$ , Incoatec) and a PILATUS 200K area detector in reflection geometry. The sample was positioned at an incident angle of  $8^\circ$  with respect to the X-ray beam and was fixed in a sample holder using a protective layer of Tyvek®. The resulting beam spot size on the sample was c. 2 mm x 0.3 mm (hor. x vert.). An optical microscope was used to accurately position the sample; a three way motorized stage (XYZ) allowed careful movement of the sample. Line measurements were performed by moving the sample vertically with a step size of 0.3 mm while collecting a diffraction pattern over a period of 10s in each point. When corrosion products were detected, an additional diffraction pattern was recorded with a longer measurement time (300 to 500s) to improve the data quality.
- **$\mu$ -Raman spectroscopy:** These analyses were performed with an InVia Raman Microscope (Renishaw). The spectral range of  $100\text{-}1500\text{ cm}^{-1}$  was recorded while the laser power and measuring time were adjusted for each sample to optimise the signal to noise rate. Sample excitation was performed by means of a green (514 nm) laser and using a Leica N Plan long working distance objective (x50/0.5), resulting in a laser spot size of  $\pm 1.2\ \mu\text{m}$ . All Raman signals were detected by a Peltier cooled CCD detector. An optical microscope was used to focus the laser on the sample. The obtained spectra were compared to reference spectra from the RRUFF database.

### 2.2.2. Continuous evaluation of corrosion layers

The continuous sensors monitored the indoor corrosivity throughout different measurement campaigns in the institutes. The results of the continuous automatic in-situ measurements were immediately available for IAQ evaluation. Both ECM and OG4 systems use the corrosion classification system ISA 71.04-1985 to convert corrosion rates into corrosivity of the environment [26]. However, this classification is not sufficiently sensitive to distinguish differences in indoor environments. For museum environments, it is advised to use the corrosion classification given by ISO 11844-1 [12,16]. Table II gives an overview of the corrosion rates  $r_{\text{tl}}$  that are calculated from the corrosion rates  $r_{\text{corr}}$  as reported by ISO 11844-1 and the corresponding environmental corrosivity of the environment. These formulas are used to compare the commercial silver sensors.

**TABLE III** Corrosivity based classification of IAQ determined from the corrosion rate of silver (ISO 11844-1). Reported corrosion rates based on mass loss  $r_{\text{corr}}$  [ $\text{mg m}^{-2}\text{ a}^{-1}$ ] are converted in metal thickness loss  $r_{\text{tl}}$  [ $\text{nm day}^{-1}$ ] by considering a silver density of  $10.5\text{ g cm}^{-3}$ .

Corrosivity Category	$r_{\text{corr}}$ [ $\text{mg m}^{-2}\text{ a}^{-1}$ ]	$r_{\text{tl}}$ [ $\text{nm day}^{-1}$ ]
IC 1 (very low indoor)	$\leq 170$	$\leq 0.0444$
IC 2 (low indoor)	170 to 670	0.0444 to 0.175

IC 3 (medium indoor)	670 to 3000	0.175 to 0.784
IC 4 (high indoor)	3000 to 6700	0.784 to 1.75
IC 5 (very high indoor)	6700 to 16700	1.75 to 4.36

### 2.2.3. Visual characterization of corrosion layers

In the heritage community, it is common practice to estimate the corrosion rate by visual observation. Such qualitative analysis is often facilitated by using a reference area obtained by partially protecting the coupon with tape [27]. However, the visual assessment of a corroded surface is the result of a convolution of the visual appearance with a personal appreciation of its appearance (i.e., esthetical value). Because this appreciation varies between people, two quantifiable aspects of visual appearance (i.e., colour and gloss) were used for the evaluation of degradation of the UAC coupons. The colour change and loss of gloss on coupons that were exposed for 3 months in various locations in the 3 museums were compared with electrochemical analysis to find the correlation between the assessments. To confirm if the visual appearance measurement are valuable as corrosion rate assessment, the impact of position and orientation of the sensors on the colour values were evaluated. The impact of coupon orientation was estimated by placing a UAC coupon at 5 sides of a Plexiglass cube (50 cm x 50 cm x 50cm). In a second setup, 3 UAC coupons were placed in close proximity to each other and positioned in the same direction to evaluate the reproducibility. In the third setup, 4 coupons were distributed throughout a room. For all coupons the front and backside 3-point averages were measured. The following instruments were used for the gloss and colour measurements:

- **Change in gloss:** This is measured with an Elcometer 406 Novo-gloss Lite™ miniature gloss meter (X-rite). The reflectance is expressed relative to an ideal reflecting diffuser at an angle of incidence of 60° in gloss units (GU). The change in gloss is described by the reflectance of the corroded surface, obtained by procedure NBN EN ISO 8891:2000 [28], divided by the original reflectance prior to corrosion. The measurements are in agreement with BS EN ISO 2813:2000, DIN 67530 [29,30]. (2000)
- **Change in colours:** L\*a\*b\*-values (CIELAB) are collected with an Avantes spectrophotometer consisting of an AvaLight-D(H)-S Bal light source combining a halogen-tungsten lamp for IR and visible light and a deuterium lamp for UV-light in combination with an Avaspec-2048 spectrometer (Avantes BV). Light source and detectors are coupled to a 50 mm integrating AvaSphere using fibre-optic cables. The surface is illuminated at an angle of incidence of 8°, while the diffusely reflected light is measured at 90°. The surface colour of 5 mm diameter zones are determined. The colour difference  $\Delta E$  between original and corroded surface state is calculated as the Euclidean distance  $dE_{ab}^{*76}$  (CIE DS 014-4.3/E:2007) [31].

## 3. Results

The results per approach are discussed in the following paragraphs.

### 3.1 Chemical characterization of corrosion layers

In the first approach, the aim is to explore the contribution of chemical characterization to corrosion rate assessments. To study this, an UAC coupon is exposed in the storage facility at FIN for a period of 9 months. The surface is characterized by means of a multi-analytical approach. The results are shown in Fig. 1. A visual inspection of the coupon clearly shows that the corrosion layer is inhomogeneous with more extensive corrosion at the edges. The peak in LSV (Fig. 1a) starting at -1.15 V/MSE can be attributed to acanthite ( $Ag_2S$ ) [32]. XRD measurements (Fig. 1b) confirm the presence of  $Ag_2S$  at the edge of the coupon, where the black tarnish is most striking. With SEM-EDX

an enriched sulfur content is visible at the edge (Fig. 1c). Since chlorargyrite (AgCl) is not identified with XRD on the indoor coupon, the peak in the X-ray spectrum at the Cl-K $\alpha$  position must be attributed to Ag-L lines. The  $\mu$ -Raman spectra 1 and 2 (Fig. 1d) result from the burning of the corrosion layer. The photo degradation due to the Raman laser is confirmed with optical microscopy, showing brown spots in the corrosion layer. The signal at 243 cm $^{-1}$  and the peaks at 490 cm $^{-1}$ , 1250 cm $^{-1}$  and 1435 cm $^{-1}$  are attributed to photo-decomposition products of Ag $_2$ S [33]. All chemical characterization techniques confirm the formation of Ag $_2$ S as the only corrosion product on coupons exposed to the indoor environment. This finding makes conversion between the corrosion rates in Table II possible.

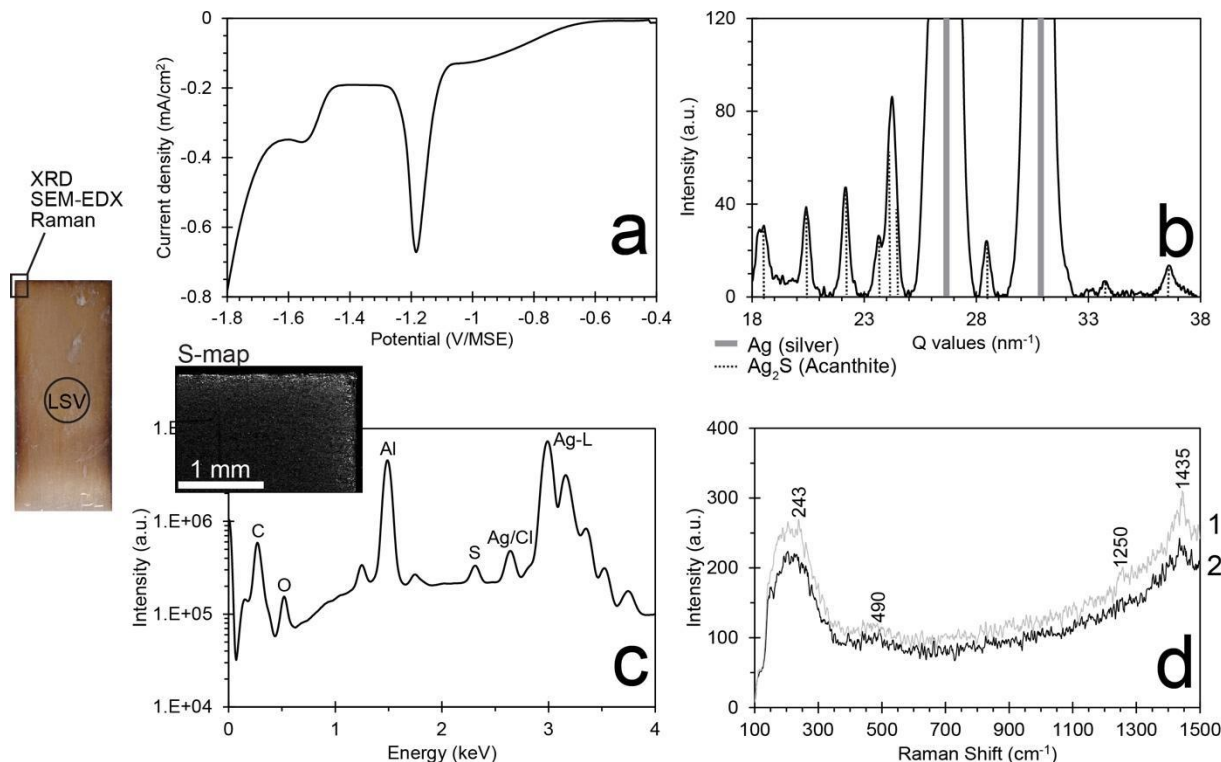


**Fig. 1** Multi-analytical characterisation of the UAC coupon exposed to the storage facility at FIN for 9 months. a) LSV analysis of the brown corrosion layer demonstrating the presence of Ag $_2$ S; b) XRD analysis confirming the LSV analysis; c) SEM-EDX analysis showing the presence S in the X-ray spectra (Al is due to the sample holder) and the enhanced corrosion at the borders as can be seen in the X-ray map of S; d) Raman spectra showing the photo degradation products of Ag $_2$ S.

For coupons exposed to an indoor environment for just 3 months at FIN only electrochemical analysis was able to detect the corrosion layers. XRD, SEM-EDX and  $\mu$ -Raman have resulted in a rather limited amount of information for these coupons. XRD is not able to detect the presence of sulphides while for SEM-EDX the sulphur content remains below detection limit. Only for the coupons exposed to an outdoor environment, the presence of chlorargyrite (AgCl) could be identified with XRD. Also LSV is able to detect the presence of AgCl (i.e., as a small peak at -0.4 V/MSE).

The evaluation of environmental corrosivity preferentially requires short exposure times and fast corrosion rate assessments. Based on the results it can be concluded that for indoor environments, electrochemical analyses seem to be more appropriate than the other analytical techniques. Therefore, electrochemistry, and more specific POT, to compare the corrosivity of locations in one museum. The corrosion assessment of the coupons exposed for a period of 3 months at different locations at FIN is shown here as an example of a corrosivity study. The chronopotentiograms (Fig. 2) clearly show differences between the locations analysed. The total reduction time ( $t_{red}$ ) is used to



calculate  $\langle r_{\text{corr}} \rangle$ . As can be seen in the table in Fig. 2, the environmental corrosivity increases from the lowest level in the display case, over the storage facility and the gallery to the outdoor environment, the latter being the most aggressive. According to the corrosivity classification of the environment in Table III, all indoor environments are rated as IC2 and the outdoor as IC3. Although the indoor locations belong to the same category, differences in corrosivity can be observed with POT.

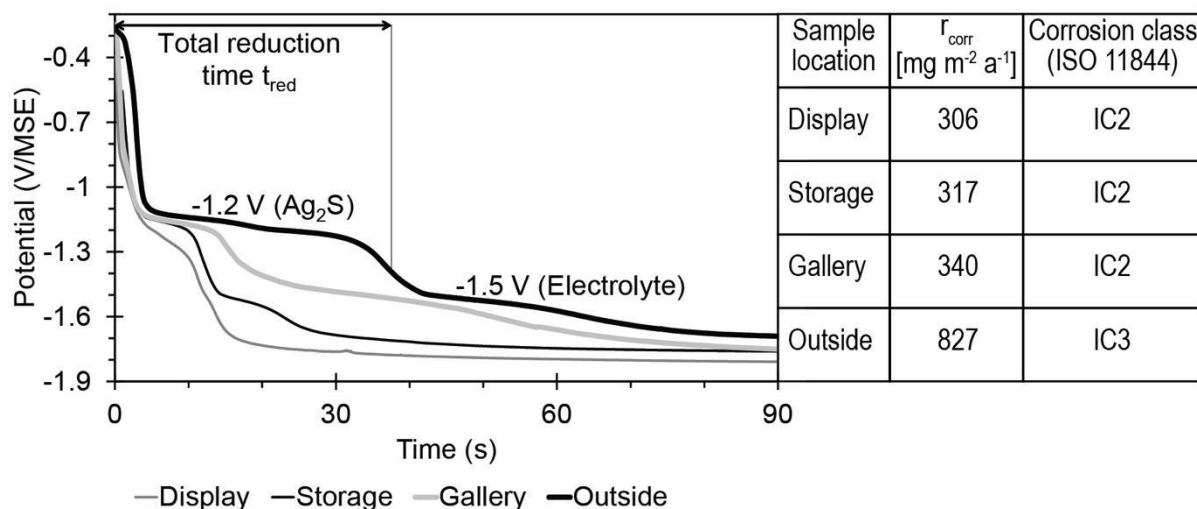


**Fig. 2** Chronopotentiograms obtained from coupons exposed at four different locations in FIN for a period of 3 months. From the total reduction time, the corrosion rate  $\langle r_{\text{corr}} \rangle$  and the corresponding corrosivity class of the environment are determined.

### 3.2 Continuous evaluation of corrosion layers

The aim of this approach is to compare corrosion rates measured with commercial sensors at different institutes. Continuous corrosion monitoring methods are able to acquire corrosion rates within shorter periods of time and to perform the analysis in-situ. Fig. 3a represents the continuous data from the resistance measurements (ECM) and mass change (OG4) for different locations in different institutes. With each displacement to another environment, the corrosion rate clearly changes. The highly sensitive ECM sensor reveals a steady corrosion build-up. On the contrary, an incidental trend is visible for the OG4 sensor, suggesting a lower sensitivity of the sensor or resolution of the analog-to-digital converter (ADC). Subtle changes in corrosion build-up ( $< 8 \text{ \AA}$ ) are not recognized by this system. For the ECM, the corrosion rate is given by the slope of the corrosion build-up. The corrosion build-up is not perfectly linear, suggesting that changes in the room or specific events can be detected. A period of c.14 days is sufficient to determine the average corrosion rate. For example, the gallery and the storage facility of ARM give a corrosion rate (i.e. slope  $\pm$  stdev) of  $0.0519 \pm 0.0001 \text{ nm day}^{-1}$  and  $0.0899 \pm 0.002 \text{ nm day}^{-1}$  respectively (Fig. 3a). Even though the difference in corrosion rate is small, it indicates a more aggressive IAQ towards silver objects in the storage facility. A follow-up study is needed to find the source of the higher corrosivity level (e.g. higher corrosive gaseous pollutants such as  $\text{H}_2\text{S}$ ,  $\text{OCS}$ ,  $\text{VOC's}$ , ...) [4, 34].

To study the intercomparability, corrosion rate assessments were also carried out with metals coupons. This was performed in the same period and in close proximity of the continuous sensors. The average corrosion rate over a period of 30 days recorded by electrochemical readout of the passive CCC coupons is almost twice as high compared to the ECM, while the CCC and UAC coupons are considerably different as well (Fig. 3b). Only the OG4 and UAC recorded a similar corrosion rate. This means that the measured corrosion rate is affected by the method itself.

Therefore, relative comparisons are only possible when similar methods are used. Consequently, it is recommended to cut coupons from the same sheet of metal.

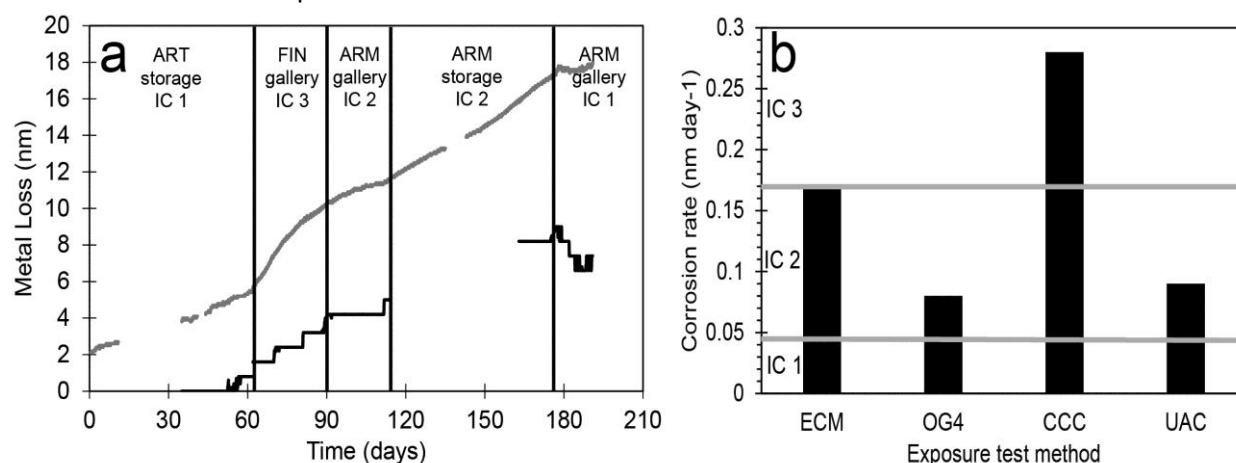


**Fig. 3** a) Metal loss of silver sensors as determined by ECM and OG4, placed parallel, in ART, FIN, ARM for a total period of 200 days. The corrosion rate is given by the slope; b) Average corrosion rate ( $r_{fil}$ ) over a period of 30 days, derived from total metal loss divided by amount of days, for 4 different corrosion monitoring methods performed in close proximity in a gallery at FIN.

### 3.3 Visual characterization of corrosion layers

The extent of corrosion can easily be observed from the change in visual appearance. However, section 3.1 demonstrated that the corrosion layer responsible for this change is extremely thin and hard to characterize with for example SEM-EDX. Also, the approved assessment with electrochemical techniques cannot be performed in-situ. This approach explores the possibilities of quantitative determination of the change in colour and change in gloss as a corrosion rate indicator by comparing them with the corrosion rates  $\langle r_{corr} \rangle$  derived from chronopotentiograms obtained at the front side of UAC coupons. A correlation of  $R^2 = 0.77$  is observed for the colour change versus  $\langle r_{corr} \rangle$  in Fig. 4a. The environments rated as corrosion category IC 2 ( $dE_{ab} < 20$ ) and IC 3 ( $dE_{ab} > 20$ ) can clearly be distinguished. However, the colour change analysis is less sensitive to subtle differences in environmental corrosivity compared to the electrochemical analysis. For gloss, on the contrary, no correlation could be found with  $\langle r_{corr} \rangle$  (Fig. 4b). The abrasion of the surface with a fibreglass brush must have a larger impact on the gloss than the corrosion process itself. On some surfaces a higher gloss is measured compared to the reference coupon.

Additionally, the impact of position and orientation of the sensors on the corrosion rates derived from colour change analysis were evaluated. After exposure, the relative standard deviation (rel. stddev) between the  $\Delta E'76$  of colour values from at least three coupons was calculated, shown in Fig. 4c. The corrosion extent appears to be reproducible when 3 coupons are placed in close proximity to each other and positioned in the same direction (with a rel. stddev of 3%). The colour of 4 coupons distributed in various positions in one room results in a much higher variation (rel. stddev = 17%). To test the effect of the coupon orientation, 5 coupons were placed on 5 sides of a Plexiglass cube (50 cm x 50 cm x 50cm). A large variation (rel. stddev = 35%) is observed. Finally, the difference between the front and backside of 17 inclined coupons was considered, resulting in a large variation (rel. stddev = 40%) [7]. Although the experimental setup is limited, this means that coupon orientation has to be chosen carefully and that air flow must be considered when estimating environmental corrosivity. Furthermore, a measuring location should not be considered as a point in a room but as a vector, taking the positioning of the coupon into account.

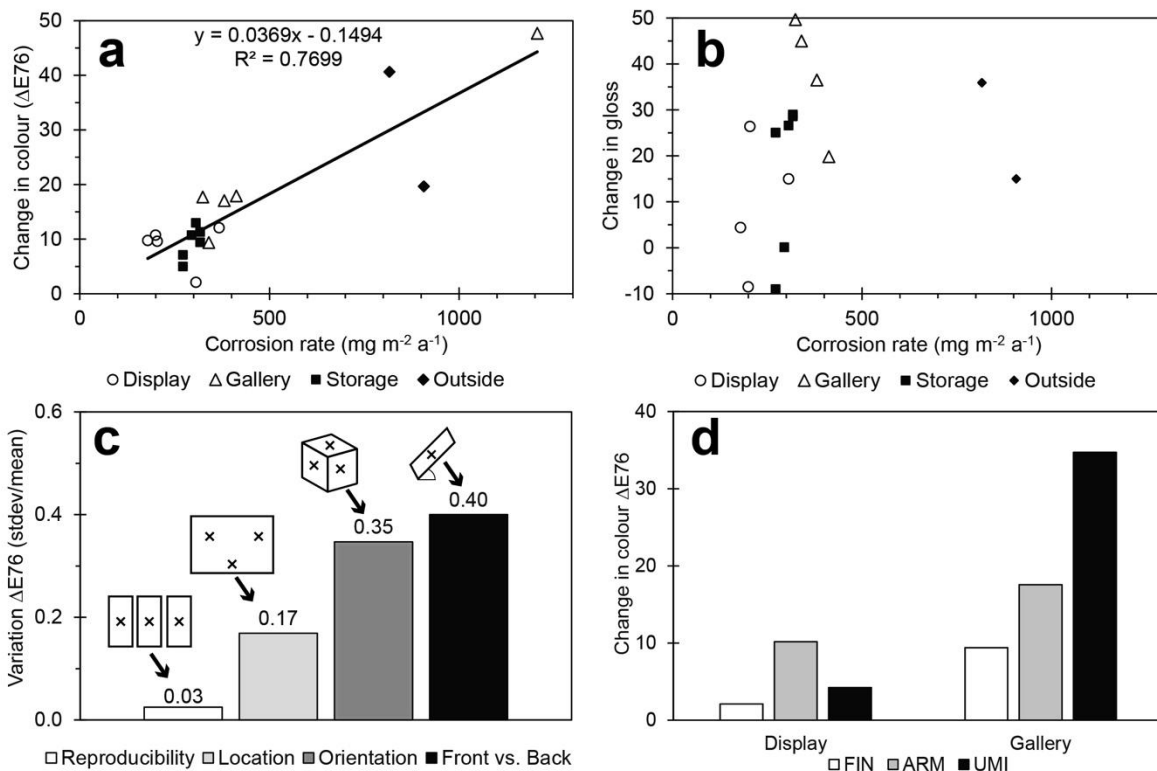


**Fig. 4** a) Relation between change in colour ( $\Delta E'_{76}$ ) and the corresponding corrosion rate ( $r_{\text{corr}}$ ) of 17 silver coupons at different locations in 3 museums for 3 months; b) Relation between change in gloss and corrosion rate ( $r_{\text{corr}}$ ) of same coupons; c) Effect of several parameters on the colour change: reproducibility of the results at the same location, effect of sample location in a room, coupon orientation and front or backside of an inclined coupon d) Protective property of the display cases in 3 different museums determined by the colour change on the front side of coupons.

The colour evaluation method is tested in a small study concerning the protective efficiency of several display cases. Fig. 5d shows that the environment inside the display cases is less aggressive than that of the galleries in which they are located. ARM has the highest display:gallery ratio (0.6), meaning that the historical oak display cases of the early 20th century are not very protective. The low protectiveness might be explained by the presence of internal sources (e.g., it is known that wood off gases VOC's [35] and silver is sensitive to this pollutant) or its high air exchange rates (around  $15,2 \text{ AE day}^{-1}$ )\* allowing the diffusion of corrosive gases from the gallery into display case [15,36,37]. UMI has a high corrosivity in the gallery. However, its modern display cases efficiently block the external pollutants from entering the cases, resulting in a high protectiveness (display:gallery ratio of 0.1). From these first results it seems possible to use colour evaluations as a quick analysis for the environmental corrosivity levels.

#### 4. Conclusion

Metal coupons are often used by heritage caretakers to evaluate the corrosivity of a given artefact environment. The problem with this method is that it requires long exposure times (up to 3 months) and that environmental corrosivity is often assessed by visual inspection by eye of the appearance of the surfaces. In this study, alternatives were explored to determine the corrosion rate.

\*The AER measurements were carried out in oaken display cases by measuring the decreasing  $\text{CO}_2$  level in the display case after filling it with gas, following the procedure described in [38].

Although the visual appearance of the coupons has changed drastically during the exposure period, measurements with SEM-EDX, XRD or  $\mu$ -Raman spectrometry have resulted in a rather limited amount of information. Micro-surface analytical techniques are only usable for coupons exposed to low corrosive indoor environments for at least 9 months in order to have corrosion layers available with sufficient thickness. Although the long exposure time makes this approach impracticable, they could confirm that the corrosion layer consists of mainly one corrosion product:  $\text{Ag}_2\text{S}$ . This information is needed to convert the one type of corrosion rate to another type. Electrochemical measurements appeared to be very effective as corrosion assessment. Also colour change measurements could be used to estimate corrosion rates but were less sensitive than the electrochemical analyses. The corrosivity could be assessed simultaneously in different locations by placing coupons cut from the same metal sheet. The resulting average corrosion rate could be determined after an exposure time of 2 to 3 months. An alternative to metal coupons is regular displacing a continuous sensor so that several locations can be assessed in a limited period of time. For the continuous monitoring in indoor situations, the ECM was able to distinguish low corrosion rates and to detect sudden changes in corrosivity (i.e., harmful events). The ECM sensor a period of c. 14 days was sufficient to determine the average corrosion rate. The ISA classification system, used by the ECM to compare corrosion rates with IAQ, appeared to be too broad for indoor situations. Consequently, the ISO 11488-1 classification was used instead. The results of the different-corrosion rate assessments are hard to mutually compare with each other due to differences in interaction between metal and environment (e.g., surface roughness, metallographic structure, etc.) and to the different methods used to determine the corrosion rate. Concluding, a relative comparison of corrosivity between different environments can only be performed on condition that similar corrosion rate assessments are used.

The results demonstrated that most indoor air situations were low corrosive (IC1 and IC2), a non-alarming corrosion rate for museum environments. The environment inside and outside display cases can often be ranked within the same class, but with metal coupons analysed with electrochemical analysis and with automatic monitoring, using the ECM system, it is possible to distinguish subtle differences in corrosivity within that class. However, orientation of the metal sensors relative to air movements tremendously affects the results. This means that air displacement should not be omitted when the indoor air quality is to be monitored.

## **Acknowledgements**

This research has been sponsored by the Belgian Federal Public Planning Service Science Policy (BELSPO) under project number BR/132/A6/AIRCHECQ. In this project an innovative monitoring kit is developed that continuously and simultaneously measures both environmental parameters and material behaviour, enabling the study of the cause-effect relationships. The Quanta 250 FEG microscope at the University of Antwerp was funded by the Hercules foundation of the Flemish Government

## **References**

1. ASHRAE, Museums, Galleries, Archives, and Libraries ASHRAE Handbook (I-P Edition), (ASHRAE Inc., Atlanta, US, 2011)
2. BIZOT green protocol (BIZOT group, New York, US, 2014)
3. D. Camuffo, in Basic environmental mechanisms affecting cultural heritage. Understanding deterioration mechanisms for conservation purposes, ed. By D. Camuffo, V. Fassina, J. Havermans (COST Action D 42: ENVIART, Nardini Editore, Firenze, Italy, 2010) p. 7

4. H.A. Ankersmit, H.T. Norman, S.F. Watts, *Atmos Environ* 39, 695 (2005)
5. V. Costa, *Reviews in Conservation* 2, 19 (2001)
6. ASHRAE Guideline 27P, (ASHRAE Inc. 2015)
7. V. Costa, M. Dubus, in *Museum Microclimates*, ed. By T. Padfield, K. Borchersen (National Museum of Denmark, 2007) pp. 63-65
8. ASTM G1-90, in *Annual Book of ASTM Standards 2001*. Vol. 03.02. (ASTM International, West Conshohocken, PA, US, 2001b) pp. 15–22
9. ASTM G4-95, in *Annual Book of ASTM Standards 2001*. (ASTM International, West Conshohocken, PA, US, 2001) pp. 45-53
10. E. Sacchi, C. Muller, *ASHRAE J* 47, 8, 40 (2005)
11. J. Tidblad, in *Corrosion and Conservation of Cultural Heritage Metallic Artefacts*, ed. By P. Dillman, G. Béranger, P. Piccardo, H. Matthiesen (CRC Press, New York, 2007) p. 37
12. ISO 11844-1, 5637-47 (International Standard Organization, Genève, Switzerland, 2006)
13. S. Capelo, P.M. Homem, J. Cavalheiro, I.T.E. Fonseca, *J Solid State Electro* 17, 223 (2013)
14. B. Ankersmit, The protection of silver from tarnishing: The use of silver tokens (SILPROT). (Indoor Air Pollution meeting, ICN, Amsterdam, the Netherlands, 26-27 August 1999), [http://www.iaq.dk/iap/iap1999/1999\\_07.html](http://www.iaq.dk/iap/iap1999/1999_07.html). Accessed 1 June 2016
15. M. Dubus, *Stud Conserv* 55, 121 (2010)
16. M. Dubus, T. Prosek, *e-Preservation Science* 9, 67 (2012)
17. T. Prosek, M. Kouril, M. Dubus, *Stud Conserv* 58, 2, 118 (2013)
18. T. Prosek, Protection of cultural heritage by real-time corrosion monitoring. (MuseCorr, 2015), <http://www.musecorr.eu/index.html>. Accessed 1 May 2015
19. N. Sridhar, D.S. Dunn, C.S. Brossia, G.A. Cragolino, and J. R. Kearns, *Corrosion tests and standards*, 2nd edition, ed. By R. Baboian (ASTM International, West Conshohocken, PA, US, 2005), pp. 206, 225
20. ISO 11844-2, (International Standard Organization, Genève, Switzerland, 2006)
21. ASM G102-89, in *Annual Book of ASTM Standards 2001*. Vol. 03.02. (ASTM International, West Conshohocken, PA, US, 1994) pp. 416-422
22. R. Bowman, Technical Note No: C.ER.GC.090705.1.0. (Rohrback Cosasco Systems, Doraville CA, US, 2014) [http://www.cosasco.com/documents/Environmental\\_Corrosion\\_Monitoring\\_Purafil.pdf](http://www.cosasco.com/documents/Environmental_Corrosion_Monitoring_Purafil.pdf), Accessed 21 Nov 2014
23. ASTM B808-05 (ASTM International, West Conshohocken, PA, US, 2005)
24. ASTM B826-97 (ASTM International, West Conshohocken, PA, US, 1997)
25. V.M. Mecea, *Sensor Actuator A-Phys* 128, 270 (2006)
26. ISA 71.04-1985 (International Society for Automation, North Carolina, US, 1985)
27. C.M. Grzywacz, *Monitoring for gaseous pollutants in museum environments*. (Getty Conservation Institute, Los Angeles, 2006) pp. 63
28. NBN EN ISO 8891:2000 BSI (Bureau voor Normalisatie, Brussel, Belgium, 2000)
29. BS EN ISO 2813, (International Standard Organization, Genève, Switzerland, 2014)
30. DIN 67530: 1982-01 (Deutsches Institut für Normung e. V., Germany, 1982)
31. CIE DS 014-4.3/E:2007 (CIE Central Bureau, Vienna, Austria, 2007)
32. H. Lin, G.S. Frankel, W.H. Abbott, *J Electrochem Soc* 160, 8, C345-C355 (2013)
33. I. Martina, R. Wiesinger, D. Jembrih-Simbürger, M. Schreiner, *e-Preservation Science* 9, 1-8 (2012)
34. M. Striegel, *The effects of low concentrations of gas phase formaldehyde on some inorganic materials found in museums*, In *AIC Objects Specialty Group, Postprints 1991 Vol. 1*, ed. By P. Hatchfield, (Washington D.C., U.S.: The American Institute for Conservation of Historic and Artistic Works, 1992) p. 1-12
35. J. Tétréault, E. Cano, M. van Bommel, *Stud Conserv* 48, 1-6 (2003)
36. L.T. Gibson, C.M. Watt, *Corrosion Science* 52, 172 (2010)

37. T. Padfield, Air Exchange Rate. (Conservation Physics, 2014)  
<http://www.conservationphysics.org/airex/air-exchange-moisture-buffer.pdf>. Accessed 24 February 2016
38. A. Calver, H. Andy, D. Thickett, S. Weintraub, *Simple methods to measure air exchange rates and detect leaks in display and storage enclosures*, In Icom Committee for Conservation, 14<sup>th</sup> triennial meeting, (The Hague, The Netherlands, 2005) p. 597-609